



Treatment of wastewater containing imazalil by means of Fenton-based processes

Dunia E. Santiago*, J. Araña, O. González-Díaz, E. Henríquez-Cárdenes, J.A. Ortega-Méndez, E. Pulido-Melián, José M. Doña-Rodríguez*, J. Pérez-Peña

Grupo de Fotocatálisis y Espectroscopía Aplicada al Medioambiente-FEAM (Unidad Asociada al ICMSE, C.S.I.C.), CIDIA-Dpto. de Química, Edificio del Parque Científico Tecnológico, Universidad De Las Palmas De Gran Canaria, Campus Universitario de Tafira, Las Palmas 35017, Spain, emails: dsantiago@proyinv.es (D.E. Santiago), jaranaesp@hotmail.com (J. Araña), ogonzalez@dqui.ulpgc.es (O. González-Díaz), ezequielhc@outlook.es (E. Henríquez-Cárdenes), jaortega@gmail.com (J.A. Ortega-Méndez), elisendapm80@hotmail.com (E. Pulido-Melián), j.dona@dqui.ulpgc.es (J.M. Doña-Rodríguez), jperez@dqui.ulpgc.es (J. Pérez-Peña)

Received 24 November 2014; Accepted 9 June 2015

ABSTRACT

This work studies the elimination, mineralization and detoxification through Fenton-based processes of wastewaters contaminated with the fungicide imazalil as a result of the postharvest treatment of bananas. Fe(II) and H₂O₂ concentrations were optimized for degradation of the corresponding imazalil concentrations. The activity of the imazalil degradation process was studied in deionized water and in simulated and real agro-industrial wastewaters. Results show that the water matrix had no detrimental effect on wastewater treatment when using the Fenton technique, but optimal iron content had to be increased when applying the photo-Fenton process. Even so, the optimal iron and H₂O₂ contents required for the photo-Fenton reaction were 6 times and 50% lower, respectively, than for the Fenton procedure. Solar pilot plant tests confirmed the detoxification of two agro-industrial wastewater effluents containing imazalil.

Keywords: Wastewater; Fenton; Imazalil; Banana postharvest; Ions

1. Introduction

The banana fruit is typically subjected to a postharvest treatment which comprises a two- or three-step washing procedure to remove dirt that might have been brought with the fruit from its growing area. A fungicide mixture is also applied to combat possible diseases that may affect the fruit. The most commonly used fungicide is imazalil [1]. Legislation has been established by many countries to control maximum

contaminant levels (MCLs) in wastewater, and these are normally set at 0.05 mg L⁻¹ for pesticides [2].

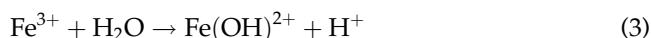
Conventional, biologically-based wastewater treatment plants are unable to eliminate fungicides due to the low biodegradability of these pollutants [3]. Advanced oxidation techniques are based on the generation of oxidizing free radicals, especially hydroxyl radicals, and constitute an option for the elimination of these substances. Among these techniques, heterogeneous TiO₂-based photocatalysis has proven to be an efficient alternative for the degradation of fungicides, although the presence of inorganic ions and

*Corresponding authors.

bacteria in the water matrix has shown to greatly influence the removal efficiency of target pollutants [4–6]. Very few studies have been carried out on imazalil degradation using advanced oxidation techniques and the papers that have been published deal for the most part with the degradation of imazalil in deionized water (DW) or only for very low concentrations [7–11]. The removal of imazalil in an agro-industrial wastewater matrix was shown to be feasible by heterogeneous photocatalysis only under certain conditions [12]. In view of the above, this article examines the possible use of alternative methods for a more practical and simple treatment procedure for such wastewaters. The techniques considered for this study are based on Fenton and photo-Fenton processes.

In the homogeneous Fenton reaction, the generation of hydroxyl radicals is obtained through the decomposition of hydrogen peroxide by the oxidation of dissolved ferrous ions, according to *reaction 1*. Fe(III) can be reduced by reaction with excess H₂O₂ to form ferrous ion again as well as additional radicals through *reaction 2*, though its reaction rate is very slow.

In the presence of UV light, the reaction becomes catalytic and the ferric ions produced in *reaction 1* are photo-reduced back to ferrous ions following *reactions 3 and 4*, leading to a greater generation of free radicals. This basically constitutes the photo-Fenton process [13,14].



The photo-Fenton process has proven to be effective for the treatment of water containing different contaminants, including phenol, fertilizers and some pesticides and dyes [15–18].

The objective of this study was the optimization of the removal of imazalil from an industrial wastewater effluent by means of Fenton-based processes.

2. Materials and methods

2.1. Reagents/chemicals

The imazalil (C₁₄H₁₄Cl₂N₂O) used was the commercial Fruitgard-IS-7.5.

pH was adjusted with diluted H₂SO₄ and NaOH.

To study the effect of inorganic ions, sodium chloride (NaCl), aluminium sulphate (Al₂(SO₄)₃·18H₂O) and calcium hydroxide (Ca(OH)₂), were used as reagents (Panreac, PRS grade).

FeSO₄·7H₂O (99.0% purity) and H₂O₂ (30% w/v) from Panreac were used as Fenton reagents.

Agro-industrial postharvest wastewater samples were collected during the 2012–2013 production campaigns from banana cooperatives in Gran Canaria, Spain.

2.2. Analytical determinations

Concentrations of imazalil at different reaction times were HPLC-measured with a Supelco Discovery C18 column (25 cm × 4.6 mm ID, 5 μm particles) and an acetonitrile-10 mM KH₂PO₄ solution (45:55) with 100 mg L⁻¹ of sodium 1-octanesulfonate as mobile phase (adjusted to pH 3 with phosphoric acid), using a UV detector (λ = 225 nm). Quantification was performed by least-squares fitting. The detection and quantification limits for imazalil were 0.05 and 0.15 mg L⁻¹, respectively. The adjusted R² was 0.998.

Total organic carbon (TOC) was measured with a TOC Shimadzu L.

A Heλios UV–vis spectrophotometer (Thermo Electron Corporation) was used to determine hydrogen peroxide concentrations. The method employed involves the formation and determination of a yellow titanium(IV)-peroxide complex at 400 nm [19]. For this purpose, samples containing hydrogen peroxide were added to a 25 mL volumetric flask containing 0.1 mg L⁻¹ H₂SO₄ and 4 g L⁻¹ titanium oxalate. The determination range was 0.1–50 mg L⁻¹, expressed as H₂O₂. The detection and quantification limits were 0.32 and 3.50 mg L⁻¹, respectively. The adjusted R² was 0.998.

Dissolved iron concentrations were measured using the o-phenanthroline method [20]. The orange ferrous complex formed by this method was determined using a spectrophotometer at 510 nm. The detection and quantification limits were 0.31 and 1.05 mg L⁻¹, respectively. The adjusted R² was 0.997.

Sample toxicity was determined with the MultiTox[®] *Vibrio Fischeri* toxicity test. This bioassay was performed following the standard UNE-EN-ISO 11348-3: 1998, which describes the determination of the inhibitory effect of water samples on the light emission of *V. fischeri* (luminescent bacteria test).

Toxicity was also evaluated with the duckweed (*Lemna minor*) toxicity test [21]. Glass Petri dishes containing 12 ± 3 fronds of common duckweed (*L. minor*)

were placed under constant visible radiation (one 18-W fluorescent tube placed approximately 25 cm above the test chambers) for 96 ± 2 h in a chamber with a temperature of $25 \pm 2^\circ\text{C}$. Four replicates were used for each sample. 15 mL of sample at pH 7.5–8 and 0.15 mL of nutrient solution were added to each dish. Growth inhibition percentage (I) was calculated with respect to a control without pollutant according to: $I(\%) = 100(C-T)/C$, where C and T are the frond number mean increments for the control and sample, respectively.

Ion chromatography was used to determine ion concentrations in solution. For this purpose, a DIONEX ionic chromatograph equipped with a GP50 gradient pump, ED50 electrochemical detector and an IonPac AS11-HC column (4×250 mm) for anions and an IonPac CS12A column (2×250 mm) for cations were used. The flow rate was 1 mL min^{-1} , and aqueous NaOH (30 mM) and 20 mM metasilphonic acid were used as anion and cation eluent, respectively.

This equipment was also employed for the determination of carboxylic acids, using for this purpose an IonPac AS11-HC column (4×250 mm) and aqueous NaOH (9 mM) as eluent at a flow rate of 1 mL min^{-1} .

A GFAAS (AA240Z Zeeman) graphite furnace atomizer (Varian GTA120) and longitudinal Zeeman-effect background correction system were used to determine dissolved aluminium. A Varian hollow cathode lamp (HCL) was used at a wavelength of 396.2 nm. Atomization was held for 2.8 s at $2,500^\circ\text{C}$. The flow rate of the inert gas (argon) was 0.3 L min^{-1} . This flow was stopped during atomization. The detection and quantification limits for aluminium were 0.35 and $1.06 \mu\text{g L}^{-1}$, respectively. The adjusted R^2 was 0.9998.

Analysis of intermediates was performed with a Varian system consisting of a 212-LC binary gradient LC/MS chromatography pump fitted with a Prostar 410 HPLC autosampler and a 320-MS LC/MS/MS system (triple quadrupole) equipped with an electrospray ionisation (ESI) interface. First, a full scan was performed both in positive and negative mode in order to identify the possible photoproducts. MS analysis was carried out in positive mode using an ion spray voltage of 1.5 kV. Ionization in the ESI source was achieved using nitrogen as nebulizer (60°C , 65 psi) and drying gas (300°C , 30 psi). Collision-induced dissociation (CID) was conducted with argon as the collision gas at a fixed pressure of 2 psi. The mobile phase consisted of water containing 0.2% formic acid and 5 mM ammonium formate (pH 2.6) (eluent A) and methanol (eluent B). A linear gradient was employed from 95 to 70% of eluent A, and column re-equilibration times of 5 min were employed for the determinations. The flow rate

was $200 \mu\text{L min}^{-1}$. The column used was a Varian Pursuit UPS 2.4 C18 ($5 \text{ cm} \times 2.0 \text{ mm ID}$, particle size $2.4 \mu\text{m}$).

Total suspended solids were measured following standard EN-872, and BOD5 was determined following ISO 5815:1989 using a BOD Sensor System 10 (VELP Scientifica, Spain), and COD was determined following standard ISO 6060:1989 using an ECO6 thermoreactor (VELP Scientifica, Spain) for digestion.

Heterotrophic bacteria were determined using the Heterotrophic Plate Count (HPC) method and R2A as culture media. R2A plate count procedure followed Standard Method 9215 C (APHA, 2004) with incubation at 28°C for 7 d.

2.3. Experimental conditions

2.3.1. Reactor and light sources at laboratory scale

Degradation tests were performed in 250-mL Pyrex glass batch reactors, filled with 200 mL of the pollutant aqueous solution and different concentrations of Fe(II) as $\text{FeSO}_4 \cdot 7\text{H}_2\text{O}$ and H_2O_2 . The solution was stirred continuously at 450 rpm. A 60 W Philips Solarium HB175 equipped with four 15 W Philips CLEO fluorescent tubes with emission spectrum from 300 to 400 nm (maximum around 365 nm) and with an average irradiation power of about 9 mW was used as UV source in the photo-Fenton studies. A schematic outline of the reactor can be seen in Fig. 1 (left).

The Fenton and photo-Fenton processes were studied for initial imazalil concentrations of 50 mg L^{-1} . Tests were performed using DW, synthetic wastewater (SW) and, finally, a real wastewater sample.

2.3.2. Solar pilot plant

The optimized photo-Fenton process was studied for an agro-industrial wastewater using a solar pilot plant.

The solar experiments were carried out with a photo-reactor comprising one CPC module (total irradiated surface 0.248 m^2) inclined at 28°N (local latitude of Las Palmas de Gran Canaria, Spain), four borosilicate glass tubes (inner diameter, 30.6 mm; length, 750 mm) connected in series, one tank and one recirculation pump. Total volume of water in the reactor was 5 L, total irradiated volume was 1.8 L and flow rate was 6 L min^{-1} . A schematic representation of the pilot plant is provided in Fig. 1 (right).

Solar ultraviolet radiation was measured with a UV-A radiometer (Acadus 85-PLS) mounted on the experimental pilot plant at the same angle as the CPC. This radiometer includes an LS-3200 integrator to

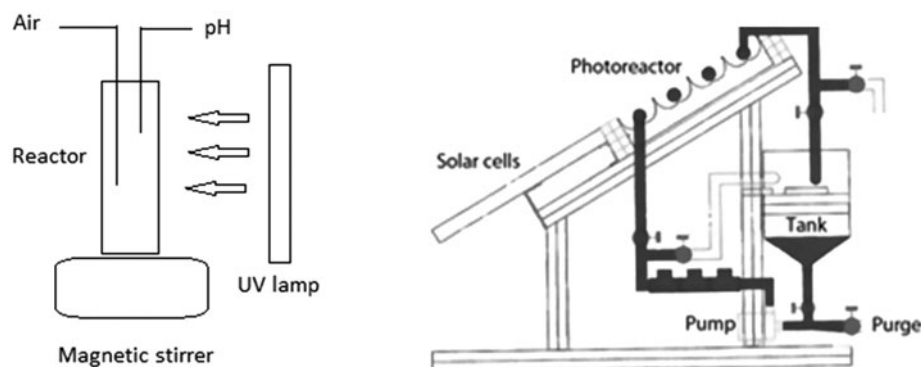


Fig. 1. Schematic representation of the reactor used for laboratory-scale experiments (left) and solar pilot plant (right).

supply the accumulated energy $E(t)$ received by the total irradiated surface of the photoreactor (in Wh). The relationship between the experiment duration time (t), the total volume of the reactor (V), the average instantaneous irradiance flux (UV), the collector surface (A) and the accumulated energy $E(t)$ is:

$$E(t) = E(t_0) + \Delta t \overline{UV} \left(\frac{A}{V} \right) \quad (5)$$

For the laboratory-scale and solar experiments, samples were taken to monitor the reaction in time intervals of 15 min during the first hour and each 30 min

thereafter. The pH of the samples was increased to 6–6.8 in order to remove dissolved iron from the solution and thus stop the Fenton reaction. The solutions were then filtered using 0.45- μm syringe filters before analysis.

3. Results and discussion

3.1. Characterization of industrial water samples

Two banana producers (hereinafter referred to as Cooperative 1 and Cooperative 2) provided wastewater samples for this study. Cooperative 1 has

Table 1

Parameters of the wastewater samples collected from the collaborating industrial facilities and MCLs in Spain

Parameters	Sample 1	Sample 2	Sample 2 -Pretreated-	MCL for reuse [2]	MCL for disposal
Imazalil (mg L^{-1})	45.20	9.40	9.53	0.05	0.05
pH	4.02	7.60	4.55	6.5–8.5	5.5–9.5
TSS (mg L^{-1})	39	124	13	80	1,200
BOD ₅ (mg L^{-1})	15	14	12	40	1,000
COD (mg L^{-1})	93.01	297.60	27.06	160	1,600
Turbidity (NTU)	56.9	47.4	3.3	1–10	–
TOC (mg L^{-1})	27.89	71.82	9.70	–	–
Cl ⁻ (mg L^{-1})	80.3	101.0	100.0	2000	300
SO ₄ ²⁻ (mg L^{-1})	298.6	219.5	319.1	2000	350
textNO ₃ ⁻ (mg L^{-1})	1.9	0.1	0.2	10	20
HCO ₃ ⁻ (mg L^{-1})	< 5.08	44.20	42.81	–	–
Total P (mg L^{-1})	0	0.13	0.10	10	5
Ca ²⁺ (mg L^{-1})	17.8	12.12	11.93	–	–
Mg ²⁺ (mg L^{-1})	0.4	9.26	9.12	–	–
Na ⁺ (mg L^{-1})	50.6	56.11	55.98	–	–
K ⁺ (mg L^{-1})	7.0	56.25	54.77	–	–
Al ³⁺ (mg L^{-1})	4.04	0	8.06	1	2
Total Fe (mg L^{-1})	<0.31	< 0.31	< 0.31	2	10
SAR (meq L^{-1})	3.27	3.46	3.48	6	–
Total heterotrophic bacteria (cfu/100 mL)	3·10 ³	7·10 ²	1·10 ²	0 ^a	–

^aThis corresponds to the most restrictive limit. Up to 10,000 cfu/100 mL may be authorized depending on the use to be given to the treated water.

an annual banana production of 10,000 tonnes and generates 63 m³ of wastewater per week. The corresponding values for Cooperative 2 are 2,400 tonnes per year and 10 m³ per week.

The mean values of the most important parameters of the wastewater samples and the corresponding MCLs for wastewater disposal [22] and reuse in crop irrigation [2] in the particular case of Spain are listed in Table 1.

Though the two collaborating cooperatives work in very different ways, both use imazalil as postharvest fungicide.

For postharvest treatment, Cooperative 1 uses well water treated by a small reverse-osmosis system. A three-step washing process is performed and imazalil is only applied in the third washing step. A considerable amount of aluminium sulphate is used to flocculate the particles of dirt washed away from the fruit and thus delay the need to renew the wash water. Of total wastewater production, only 4 m³/week contains imazalil.

Cooperative 2 uses tap water and their postharvest treatment involves a two-step process. Imazalil is added in the second step by means of a water cascade. This cooperative does not add any aluminium sulphate. In this case, the amount of wastewater containing imazalil is 2 m³/week.

Several water samples were obtained on different days from the collaborating producers. The mean parameters obtained after characterization of the wastewaters are presented in Table 1. Samples 1 and 2 correspond to Cooperative 1 and Cooperative 2, respectively.

As can be seen in Table 1, imazalil concentration can vary significantly from one agro-industrial facility to another. Nevertheless, as the detected imazalil

concentration was never above 50 mg L⁻¹, this value was taken as the working concentration for this study.

TOC and COD values were significantly higher in Sample 2 than Sample 1 wastewaters. This was most probably due to the presence of organic matter other than imazalil in Sample 2 contained in the dirt washed away from the fruit in the washing process and to the probable leaching of lignocellulose from vegetable particles. The wastewater of Cooperative 2 had a characteristic brownish colour that could indicate lignin leachate [23]. In order to reduce the organic content and dark colour of this water, a flocculation pre-treatment with aluminium sulphate was carried out [24,25]. The characterization of the water sample after this pre-treatment is included in Table 1. It can be seen that TOC, COD, total heterotrophic bacteria and turbidity were significantly reduced with this flocculation procedure, which concurs with the results of other studies [26,27].

3.2. Fenton treatment of imazalil in DW

In order to optimize the Fenton reagents required for the elimination and mineralization of imazalil, several experiments were carried out adding different concentrations of Fe(II) and H₂O₂. The duration of each test was 120 min.

Theoretically, if we assume that the oxygen necessary for the oxidation of 50 mg L⁻¹ imazalil is provided by the addition of H₂O₂, then 223 mg L⁻¹ H₂O₂ would be required. The first Fenton experiments were performed for 50 mg L⁻¹ imazalil, varying the initial concentration of Fe²⁺ between 0 and 80 mg L⁻¹ for an initial H₂O₂ concentration of 307 mg L⁻¹ (Fig. 2, left). It can be observed that mineralization increased with increasing Fe(II) up to an Fe(II) concentration of

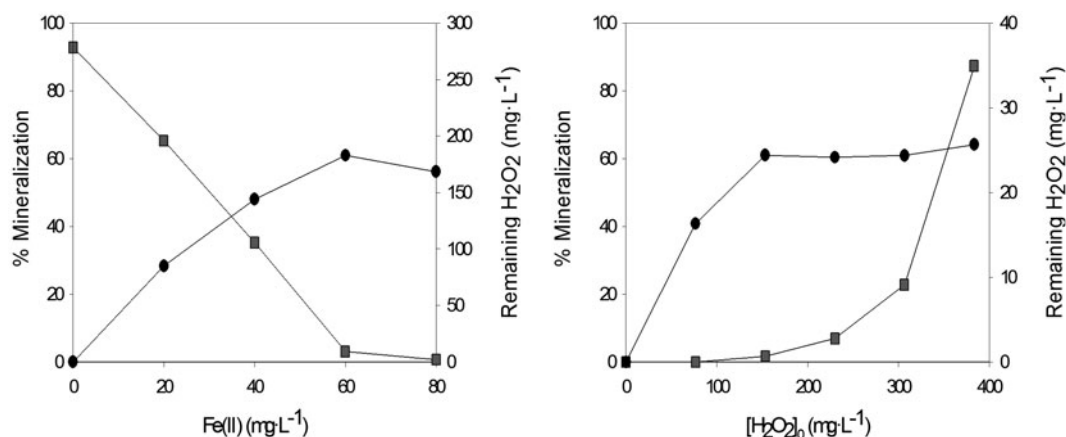


Fig. 2. % Mineralization (●) and remaining H₂O₂ (■) for the removal of 50 mg L⁻¹ imazalil in DW at natural pH (pH₀ 3.8) via Fenton using different concentrations of Fe(II) (left) and H₂O₂ (right) with reaction time 120 min.

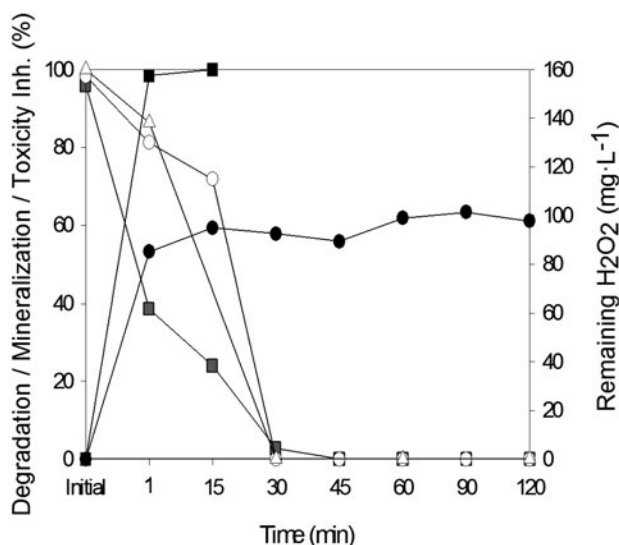


Fig. 3. H_2O_2 (■), IMZ (■), TOC (●) and toxicity to *V. fischeri* (○) and *L. minor* (△) during the Fenton treatment of a 50 mg L^{-1} imazalil aqueous solution at natural pH (pH_0 3.8) using initial concentrations of 60 mg L^{-1} Fe(II) and 153.45 mg L^{-1} H_2O_2 .

60 mg L^{-1} . For higher Fe(II) loads, mineralization remained constant. Imazalil degradation rates are not given because in all cases imazalil elimination was achieved instantly after addition of the two Fenton reagents.

The experiments were repeated employing a constant concentration of Fe^{2+} (60 mg L^{-1}) and with H_2O_2 concentrations varying between 75 and 400 mg L^{-1} (Fig. 2, right). In this case, mineralization reached its maximum value when 153 mg L^{-1} H_2O_2 were added.

It can be concluded that the optimized Fe(II) and H_2O_2 concentrations for the elimination of 50 mg L^{-1} imazalil are 60 and 153 mg L^{-1} , respectively. It should

be noted that no H_2O_2 remained in the solution after the process when using these amounts of Fenton reagent. In terms of sample detoxification, this is important as H_2O_2 has been shown to be a toxic environmental agent [28].

As can be seen, the optimal H_2O_2 concentration is lower than the stoichiometric for the total mineralization of 50 mg L^{-1} imazalil. This may be because complete mineralization is not attained due to the formation of persistent or stable by-products, such as acetic acid, as is detailed in Section 3.5. In this sense, it can be observed from Fig. 2 that only 60% mineralization was achieved for the optimized Fenton conditions.

Toxicity was measured at different reaction times for the optimized reaction and the results are shown in Fig. 3. It can be observed that total imazalil removal and around 60% mineralization were achieved immediately after the addition of the Fenton reagents, and that toxicity decreased with the consumption of H_2O_2 along the reaction.

3.3. Photo-Fenton treatment of imazalil in DW

As in the previous section, several experiments were carried out adding different concentrations of Fe(II) and H_2O_2 to optimize the loads for the treatment of 50 mg L^{-1} imazalil in DW. The duration of each experiment was also 120 min. It should be noted that photolysis of imazalil does not occur at the natural working pH (3.8).

First, H_2O_2 initial concentration was maintained at 307 mg L^{-1} , and Fe(II) loads were varied between 0 and 60 mg L^{-1} . The results are shown in Fig. 4 (left). Mineralization was higher than 88% for Fe(II) concentrations above 2.5 mg L^{-1} .

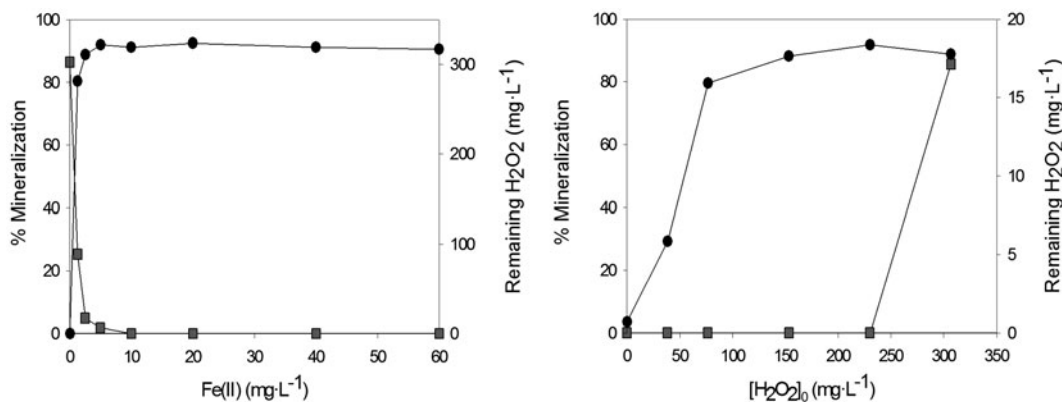


Fig. 4. % Mineralization (●) and remaining H_2O_2 (■) for the removal of 50 mg L^{-1} imazalil in DW at natural pH (pH_0 3.8) via photo-Fenton and using different concentrations of Fe(II) (left) and H_2O_2 (right) with reaction time 120 min.

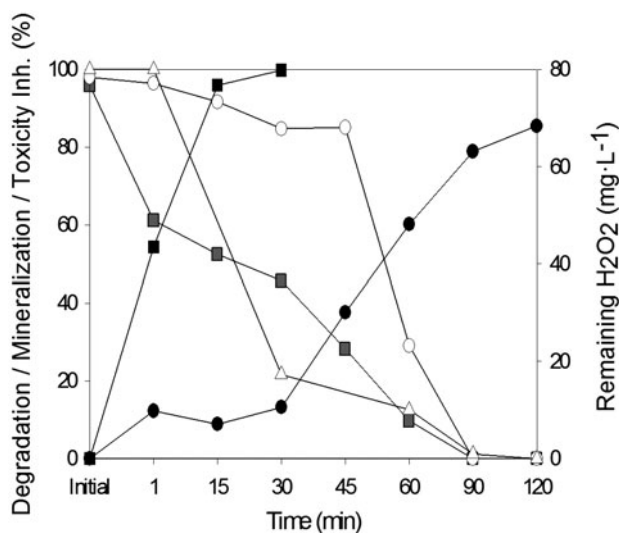


Fig. 5. H₂O₂ (■), IMZ (■), TOC (●) and toxicity to *V. fischeri* (○) and *L. minor* (△) during the photo-Fenton treatment of a 50 mg L⁻¹ imazalil aqueous solution at natural pH (pH₀ 3.8) using initial concentrations of 2.5 mg L⁻¹ Fe(II) and 76.73 mg L⁻¹ H₂O₂.

The experiments were then repeated for a constant concentration of 2.5 mg L⁻¹ Fe(II) with H₂O₂ concentrations varying between 0 and 307 mg L⁻¹. It was determined from the results shown in Fig. 4 (right) that an initial addition of 77 mg L⁻¹ H₂O₂ was sufficient to achieve 80% mineralization.

It can be concluded from these results that the photo-Fenton process requires 24 times less Fe(II) and half the H₂O₂ load compared to the Fenton procedure to achieve an optimized mineralization for 50 mg L⁻¹ imazalil in DW. In addition, mineralization was considerably higher when using the photo-Fenton technique.

Toxicity was also followed for the treatment of 50 mg L⁻¹ imazalil using the photo-Fenton process and with the optimized Fe(II) and H₂O₂ concentrations of 2.5 and 77 mg L⁻¹, respectively. Detoxification took place in this case after 90 min irradiation and coincided with H₂O₂ total consumption (see Fig. 5). It can be seen that toxicity to *L. minor* decreased faster than to *Vibrio fischeri*, which may indicate that the latter organism is more sensitive to H₂O₂.

3.4. Fenton-based treatments of imazalil in SW

For simplification purposes, the Fenton-based techniques were next studied in a SW containing 50 mg L⁻¹ imazalil, 100 mg L⁻¹ chloride (as NaCl), 300 mg L⁻¹ sulphate (as Al₂(SO₄)₃·18H₂O) and 20 mg L⁻¹ calcium (as Ca(OH)₂). This SW was used to

simulate the general inorganic composition found in the analysed wastewater samples. The resulting pH of this solution was 4.25.

Several authors have reported that pH is one of the major factors that can limit Fenton-based processes in the treatment of wastewater due to its role in the speciation of iron and the stability of hydrogen peroxide. In this respect, increasing pH above 5 leads to a decrease in the concentration of the photoactive Fe [OH]²⁺ species and leads to the precipitation of Fe (OH)₃, thus inhibiting the reaction of hydroxyl radicals [29–31]. It was therefore decided to include an assessment of the effect of pH in this study.

Due to the pH-dependent speciation of aluminium and the consequent formation of insoluble Al(OH)₃ at pH values above 4.5 [32], flocs produced in the SW at higher pH values were removed by filtration prior to the experiments.

It can be observed from the results shown in Fig. 6 that increasing the pH above 4 resulted in a sharp decrease in activity for the photo-Fenton process. This is due to the formation of the aforementioned Fe(OH)₃ and the consequent lower availability of iron to react with H₂O₂ and produce hydroxyl radicals. As a result, it was observed that remaining H₂O₂ increased with increasing pH. This effect was more notable for the treatment of the SW than the DW.

The presence of inorganic anions such as chloride and sulphate has been reported to have a significant effect on photo-Fenton mineralization.

The presence of chloride in an aqueous solution containing ferric ions results in the formation of less reactive [FeCl]²⁺ and [FeCl₂]⁺ complexes, although [Fe(OH)²⁺] is still the predominant species at pH 3.0 [33–35]. Similarly, sulphate ions can form complexes with ferrous and ferric ions, such as FeSO₄⁺. At pH 3.0, FeSO₄⁺ and Fe(OH)₂⁺ are the predominant ferric species [36].

It can be concluded that the presence of chloride and sulphate ions in the water matrix reduces the concentration of ferrous and ferric ions in the solution, and thus inhibits the photo-Fenton process.

With this in mind, the optimized Fe(II) and H₂O₂ loads were reassessed for the treatment of 50 mg L⁻¹ imazalil in SW at natural pH, that is pH 4.25, by photo-Fenton. The results, shown in Fig. 7, indicate that a fourfold increase in iron load (to 10 mg L⁻¹) was required to achieve optimum mineralization.

For the Fenton technique, mineralization was only slightly inhibited at pH 5 and 7 by the presence of ions in the water matrix (Fig. 6, left). This can be attributed mainly to the much higher iron content used for the Fenton reaction. It was observed that pH fell from 4.25 to 2.8 ± 0.1 immediately after the

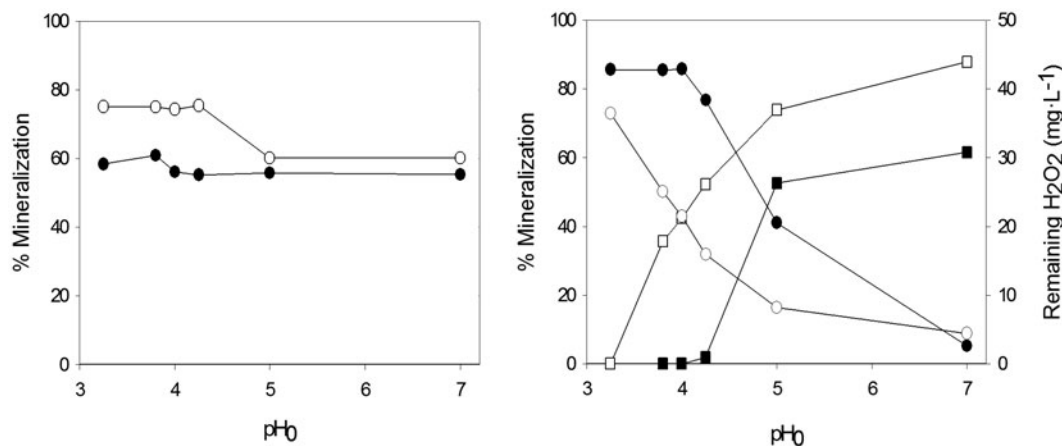


Fig. 6. % Mineralization (●,○) and remaining H₂O₂ (■,□) for the Fenton (left) and photo-Fenton (right) treatment of a 50 mg L⁻¹ imazalil aqueous solution in DW (black symbols) and SW (synthetic wastewater, white symbols) using initial concentrations of 60 and 2.5 mg L⁻¹ Fe(II) and 153 and 77 mg L⁻¹ H₂O₂, respectively.

addition of the Fenton reagents to the system. It should also be noted that H₂O₂ was totally consumed for all Fenton reactions after 120 min.

The Fenton technique was thoroughly assessed for the SW (see Fig. 8). Mineralization was notably higher at pH values below 4.25 compared to the treatment with DW (Fig. 6, left). Specifically, 61 and 74% mineralizations were obtained when applying the Fenton process to the deionized and synthetic water matrices, respectively, at the optimized reagent concentration values. However, although H₂O₂ consumption was complete after 120 min, it was slower when ions were present in the water matrix, which can be attributed to interactions taking place between the dissolved iron and the inorganic species in the solution. Total consumption of H₂O₂ coincided with complete detoxification, as also occurred with the DW treatment.

Aluminium has been reported to form complexes and precipitate in the presence of acetic and oxalic

acids at pH values above 4 [37]. The pH of samples taken from the Fenton-based reactions was increased to 6–6.8 in order to precipitate iron and remove it from the solution to stop the Fenton reaction and comply with legally determined iron limits in water [2]. Aluminium-oxalate complexes may therefore have precipitated in reactions containing dissolved aluminium, and so the TOC remaining in solution was lower for the Fenton processes when using SW. The formation of oxalic acid, among others, was followed for this reaction, and the results are discussed in Section 3.5.

3.5. Identification of photoproducts

Two complementary techniques were employed to identify the degradation pathway that results from the elimination of imazalil via Fenton and photo-Fenton methods in both DW and SW: ion chromatography

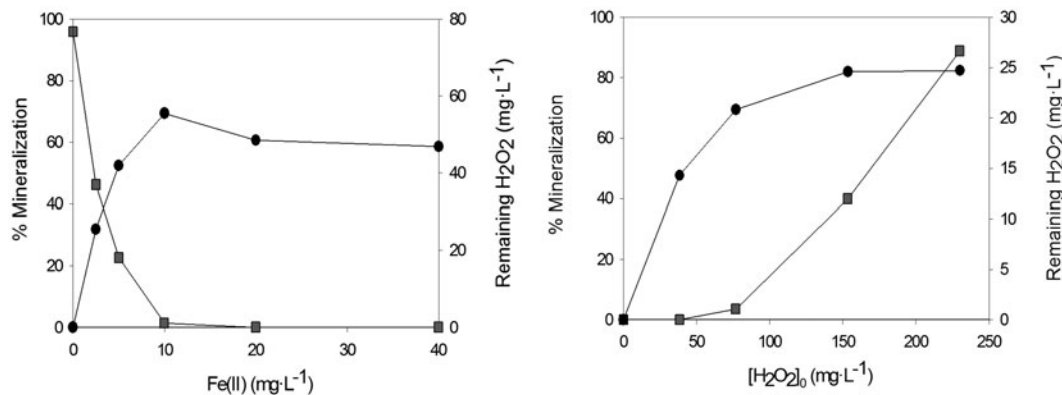


Fig. 7. % Mineralization (●) and remaining H₂O₂ (■) for the removal of 50 mg L⁻¹ imazalil in SW at natural pH (pH₀ 4.25) via photo-Fenton and using different concentrations of Fe(II) (left) and H₂O₂ (right).

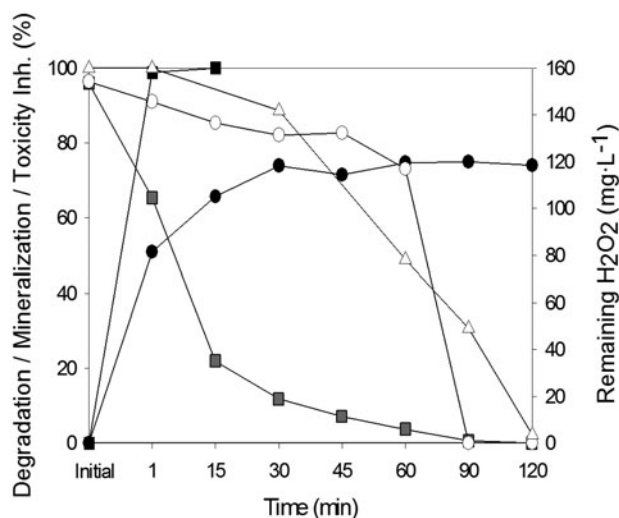


Fig. 8. H₂O₂ (■), IMZ (●), TOC (●) and toxicity to *V. fischeri* (○) and *L. minor* (△) during the Fenton treatment of 50 mg L⁻¹ imazalil in SW at natural pH (pH₀ 4.25) using initial concentrations of 60 mg L⁻¹ Fe(II) and 153.45 mg L⁻¹ H₂O₂.

and LC-MS. It was concluded from the LC-MS analyses that most of the by-products that resulted from these techniques were carboxylic acids.

The overall oxidation reaction for imazalil should produce two moles of chloride and two moles of nitrogen-containing ions per mole of imazalil. We followed the formation of these ions as possible final products of the degradation reaction. The results are shown in Fig. 9.

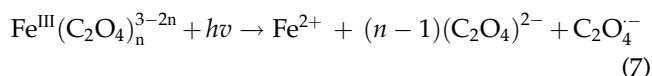
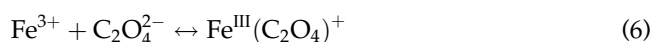
The expected amount of chloride for complete mineralization of 50 mg L⁻¹ imazalil was obtained in both the Fenton and photo-Fenton processes. This confirms a radical-nucleophilic aromatic substitution due to the liberation of chloride ions during the degradation of imazalil. Dechlorination was immediate in the Fenton process due to the high Fenton reagent concentrations employed which enables a faster production of hydroxyl radicals.

Heterocyclic nitrogen groups in imidazoles are usually converted into ammonium or nitrate ions via the formation of amines or hydroxylamines [38]. It can be seen in Fig. 9 that the release of nitrogen atoms into the solution (as inorganic nitrogen) was clearly lower than stoichiometric after 120 min. This suggests that other nitrogen-containing compounds must be present in the solution.

It was observed that the presence of ions in the water matrix delayed the release of nitrogen and chloride. This was probably due to lower iron availability in the media for the formation of hydroxyl radicals, as previously mentioned.

Regarding the production of the identified carboxylic acids, these compounds accounted for around 75% of the final TOC remaining after the treatment of imazalil using both the Fenton and photo-Fenton processes. However, the distribution of these acids differed depending on the technique used.

In this respect, the experimental results obtained in this work show that large amounts of oxalate were produced and accumulated in the DW Fenton process. However, rapid oxalate mineralization was observed for both the DW and SW photo-Fenton processes. Numerous studies have shown that oxalic acid can form photoactive complexes with Fe(II) and Fe(III) [39,40] which promote mineralization. From the results, it is concluded that the photochemical dissociation of Fe(III)-oxalate complexes by means of reactions 6–8 were responsible for the higher mineralization obtained when illumination was added to the system.



As for the Fenton reactions, it can be seen in Fig. 9 that relatively low amounts of oxalic acid were produced in the SW system compared to the DW system. This is attributed to the precipitation of aluminium-oxalate complexes formed in the SW reaction, as mentioned previously. Moreover, the 15% higher mineralization obtained for the SW system compared to the DW system (see Fig. 6) can be explained by the precipitation of around 16 mg L⁻¹ of the oxalic acid formed in the DW Fenton process.

Malonic acid concentrations of below 2 mg L⁻¹ were found in solution for both the Fenton and photo-Fenton techniques, independent of the water matrix employed. This acid is formed from ring-opening of the aromatic intermediates and has been reported to be mainly oxidized to acetic acid [41].

It should also be noted that the acetic acid that formed remained in the solution because acetic acid is refractory to further oxidation due to the low rate constant of its reaction with hydroxyl radicals [42].

3.6. Photo-Fenton of imazalil in agro-industrial wastewater

Finally, the elimination and mineralization of 50 mg L⁻¹ imazalil were performed in a real wastewater

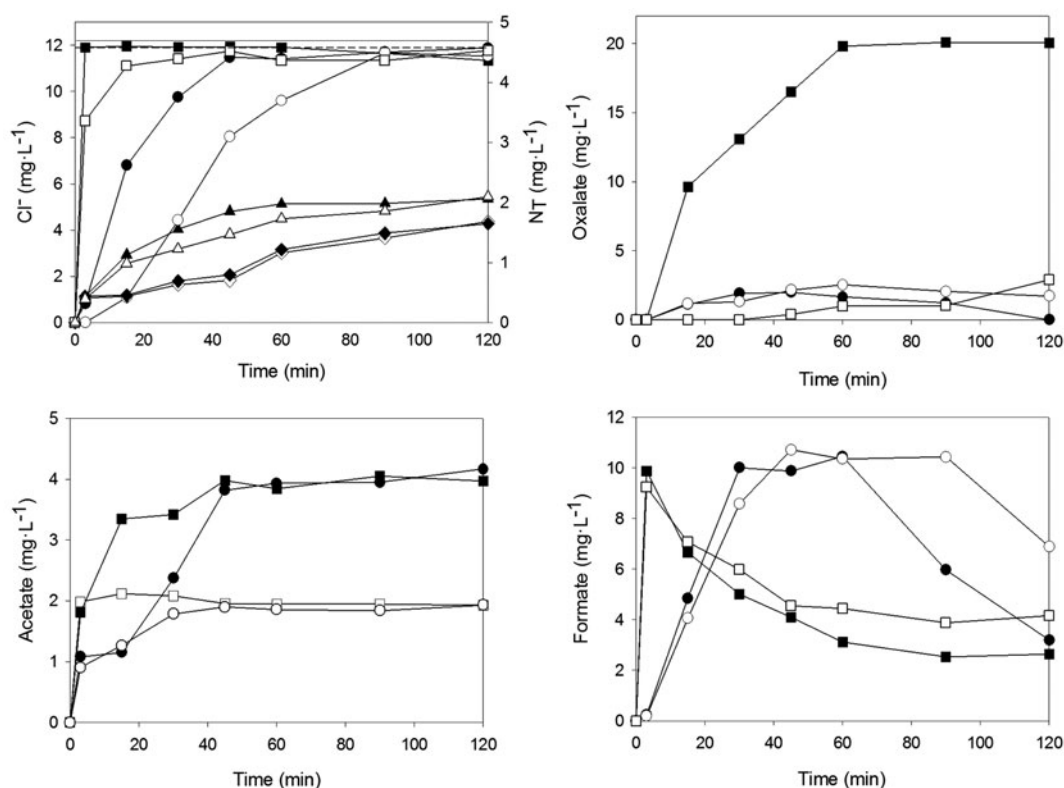


Fig. 9. Evolution of inorganic and organic ions during Fenton and photo-Fenton treatment in DW (black symbols) and SW (white symbols) and at natural pH (pH_0 3.8–4.25). Photo-Fenton data are represented by (●,○) and Fenton by (■,□). Total inorganic nitrogen is represented by (▲,△) for the Fenton reaction and by (◆,◇) for photo-Fenton. Stoichiometric chloride and inorganic nitrogen are represented by (–) and (–), respectively.

sample (Sample 1 - see Table 1), using the photo-Fenton technique and the optimized Fe(II) and H_2O_2 loads for SW, namely 10 mg L^{-1} Fe(II) and 77 mg L^{-1} H_2O_2 . Sample 1, was chosen because TOC in the sample was almost stoichiometric to the imazalil content. The results are shown in Fig. 10.

It can be seen that mineralization was less than 60% under these conditions for the real wastewater treatment, a value which is noticeably lower than for the SW treatment (see Fig. 7). This can be attributed mainly to the presence of bacteria and possible traces of turbidity in the supernatant of the wastewater sample.

It should be noted that H_2O_2 was completely consumed for the wastewater sample treatments. Increasing H_2O_2 initial concentration to 153 mg L^{-1} yields higher mineralization, but is considered undesirable due to the higher reactive consumption.

Alternatively, filtering the wastewater through a $0.45\text{-}\mu\text{m}$ filter removes bacteria and possible traces of turbidity and the application of photo-Fenton to wastewater Sample 1 after this pre-treatment and

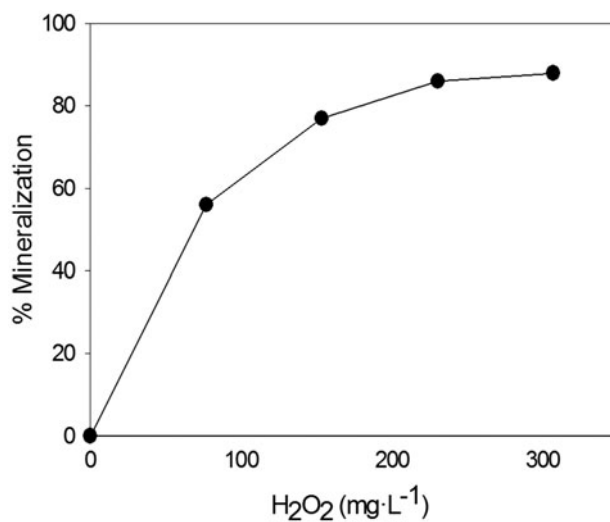


Fig. 10. % Mineralization for the removal of 50 mg L^{-1} imazalil in wastewater at natural pH (pH_0 4) via photo-Fenton and using 10 mg L^{-1} Fe(II) and different concentrations of H_2O_2 .

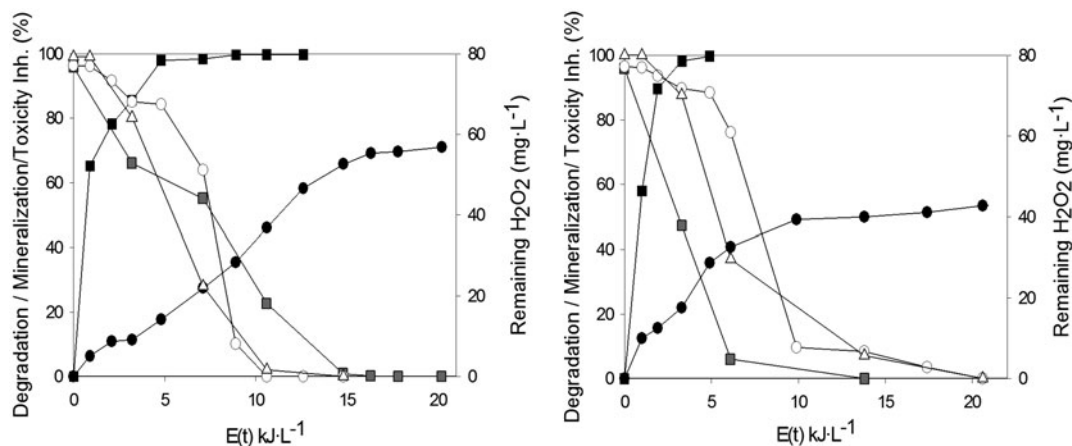


Fig. 11. H_2O_2 (■), IMZ (●), TOC (●) and toxicity to *V. fischeri* (○) and *L. minor* (△) during the photo-Fenton treatment of wastewater samples n° 1 (left) and 2 (right) containing 50 mg L^{-1} imazalil at natural pH (pH_0 4–4.55) using initial concentrations of 10 mg L^{-1} Fe(II) and 76.73 mg L^{-1} H_2O_2 .

using the optimized conditions for SW proved to be as effective as the SW treatment.

3.7. Solar pilot plant

The optimal Fe(II) and H_2O_2 concentrations determined at laboratory scale for the treatment of filtered agro-industrial wastewater containing imazalil were applied at pilot plant scale in order to validate the results.

Fig. 11 shows the degradation and mineralization profiles of imazalil against accumulated energy. It should be noted that the time necessary for the effluent containing imazalil to be treated depends to a large extent on climate conditions. Generally, it may be assumed that the average solar-UV (300–400 nm) on a perfectly sunny day for 2 h around noon is about $50 \text{ W}_{\text{UV}} \cdot \text{m}^{-2}$ at our location (Gran Canaria, Spain). Under these conditions and using the reactor shown in Fig. 1, 1 kJ L^{-1} is equivalent to 6.94 min of illumination [15].

As can be observed from Fig. 11, maximum mineralization was attained after around 15–20 kJ L^{-1} of accumulated energy, with this value corresponding to a reaction time ($t_{50\text{W}}$) of 104–139 min.

Imazalil and toxicity to *Vibrio fischeri* were completely eliminated after the solar photo-Fenton treatment and 71 and 59% mineralization were obtained for wastewater Samples 1 and 2, respectively. These results are similar to those obtained at laboratory scale.

The lower mineralization attained for the treatment of wastewater Sample 2 can be mainly attributed to the higher initial TOC and IC, which may also explain the faster H_2O_2 consumption. In this respect, bicarbonate

ions have been reported to be $\cdot\text{OH}$ radical scavengers [43].

These results confirm the feasibility of using photo-Fenton techniques to achieve a quality of water for irrigation reuse which complies with Spanish legislation for wastewater reclamation [2] (see Table 1).

It should be noted that after completion of the photo-Fenton process there remains a need to precipitate the iron(III) hydroxide using a decantation process at pH 6 in order to obtain an iron concentration within the current regulations.

4. Conclusions

Both Fenton and photo-Fenton processes offer a good option for the degradation, mineralization and detoxification of imazalil in different water matrices. Optimal concentrations of Fe(II) = 60 and 10 mg L^{-1} and H_2O_2 = 153 and 77 mg L^{-1} were determined for the Fenton and photo-Fenton processes, respectively, in DW.

Fe(II) concentration had to be increased to 10 mg L^{-1} when SW containing ions was treated at natural pH_0 . Even in that case, Fe(II) consumption was 6 times lower when applying the photo-Fenton technique compared to the Fenton treatment and only half the amount of H_2O_2 was required. The photo-Fenton process is therefore considered more suitable for the treatment of wastewater containing up to 50 mg L^{-1} imazalil.

The presence of ions reduces the amount of iron available in solution for the Fenton-based reactions to take place, particularly at pH values above 4. However, the precipitation of aluminium-oxalate

complexes formed during the SW treatment enabled higher mineralization via Fenton reaction in this water matrix when compared to the application of this technique in DW.

Solar pilot plant tests with wastewater samples provided by two different cooperatives gave similar results to those obtained at laboratory scale, with complete detoxification achieved after 20 kJ L⁻¹ accumulated energy.

Acknowledgements

We thank the Spanish Ministry of Economy and Competitiveness (MINECO, Government of Spain) for funding projects NANOBAC (IPT-2011-1113-310000) and 2010-3E UNLP10 MINECO -726 and the Universidad de Las Palmas de Gran Canaria for funding the PhD fellowship of Dunia E. Santiago.

References

- [1] M. Duque Yanes, Pudricion de corona en el plátano canario (Crown rot in the Canary Islands banana), first ed., Cooperativa Platanera de Canarias (COPLACA), Tenerife, 2004, pp. 1–38.
- [2] Boletín Oficial del Estado (BOE), Real Decreto 1620/2007, BOE, 294 (2007) 50639–50661.
- [3] J. Araña, C. Garriga i Cabo, C. Fernández Rodríguez, J.A. Herrera Melián, J.A. Ortega Méndez, J.M. Doña Rodríguez, J. Pérez Peña, Combining TiO₂-photocatalysis and wetland reactors for the efficient treatment of pesticides, *Chemosphere* 71(4) (2008) 788–794.
- [4] D.C. Schmelling, K.A. Gray, P.V. Kamat, The influence of solution matrix on the photocatalytic degradation of TNT in TiO₂ slurries, *Water Res.* 31(6) (1997) 1439–1447.
- [5] D.D. Dionysiou, M.T. Suidan, E. Bekou, I. Baudin, J.M. Lainé, Effect of ionic strength and hydrogen peroxide on the photocatalytic degradation of 4-chlorobenzoic acid in water, *Appl. Catal. B Environ.* 26(3) (2000) 153–171.
- [6] M. Pelaez, A.A. de la Cruz, K. O’Shea, P. Falaras, D.D. Dionysiou, Effects of water parameters on the degradation of microcystin-LR under visible light-activated TiO₂ photocatalyst, *Water Res.* 45(12) (2011) 3787–3796.
- [7] R. Hazime, C. Ferronato, L. Fine, A. Salvador, F. Jaber, J. Chovelon, Photocatalytic degradation of imazalil in an aqueous suspension of TiO₂ and influence of alcohols on the degradation, *Appl. Catal. B Environ.* 126 (2012) 90–99.
- [8] R. Hazime, Q.H. Nguyen, C. Ferronato, T.K.X. Huynh, F. Jaber, J. Chovelon, Optimization of imazalil removal in the system UV/TiO₂/K₂S₂O₈ using a response surface methodology (RSM), *Appl. Catal. B Environ.* 132–133 (2013) 519–526.
- [9] D.E. Santiago, J.M. Doña-Rodríguez, J. Araña, C. Fernández-Rodríguez, O. González-Díaz, J. Pérez-Peña, A.M.T. Silva, Optimization of the degradation of imazalil by photocatalysis: Comparison between commercial and lab-made photocatalysts, *Appl. Catal. B Environ.* 138–139 (2013) 391–400.
- [10] I. Carra, S. Malato, M. Jiménez, M.I. Maldonado, J.A. Sánchez Pérez, Microcontaminant removal by solar photo-Fenton at natural pH run with sequential and continuous iron additions, *Chem. Eng. J.* 235 (2014) 132–140.
- [11] S. Malato, J. Blanco, D.C. Alarcón, M.I. Maldonado, P. Fernández-Ibáñez, W. Gernjak, Photocatalytic decontamination and disinfection of water with solar collectors, *Catal. Today*, 122(1–2) (2007) 137–149
- [12] D.E. Santiago, J. Araña, O. González-Díaz, M.E. Alemán-Dominguez, A.C. Acosta-Dacal, C. Fernandez-Rodríguez, J. Pérez-Peña, J.M. Doña-Rodríguez, Effect of inorganic ions on the photocatalytic treatment of agro-industrial wastewaters containing imazalil, *Appl. Catal. B Environ.* 156–157 (2014) 284–292.
- [13] H.J.H. Fenton, Oxidation of tartaric acid in presence of iron, *J. Chem. Soc. Trans.* 65 (1894) 899–910.
- [14] F. Haber, J. Weiss, The catalytic decomposition of hydrogen peroxide by iron salts, *Proc. R. Soc. A Math. Phys. Eng. Sci.* 147(861) (1934) 332–351.
- [15] M.J. Hernández-Rodríguez, C. Fernández-Rodríguez, J.M. Doña-Rodríguez, O. González-Díaz, D. Zerbaní, J. Pérez Peña, Treatment of effluents from wool dyeing process by photo-Fenton at solar pilot plant, *J. Environ. Chem. Eng.* 2 (2014) 163–171.
- [16] S. Karthikeyan, A. Titus, A. Gnanamani, A.B. Mandal, G. Sekaran, Treatment of textile wastewater by homogeneous and heterogeneous Fenton oxidation processes, *Desalination* 281 (2011) 438–445.
- [17] M.C. Ortega-Liébana, E. Sánchez-López, J. Hidalgo-Carrillo, A. Marinas, J.M. Marinas, F.J. Urbano, A comparative study of photocatalytic degradation of 3-chloropyridine under UV and solar light by homogeneous (photo-Fenton) and heterogeneous (TiO₂) photocatalysis, *Appl. Catal. B Environ.* 127 (2012) 316–322.
- [18] A. Akyol, O.T. Can, E. Demirbas, M. Kobya, A comparative study of electrocoagulation and electro-Fenton for treatment of wastewater from liquid organic fertilizer plant, *Sep. Purif. Technol.* 112 (2013) 11–19.
- [19] R.M. Sellers, Spectrophotometric determination of hydrogen peroxide using potassium titanium(IV) oxalate, *Analyst* 105 (1980) 950–954.
- [20] L.G. Saywell, B.B. Cunningham, Determination of iron: colorimetric o-phenanthroline method, *Ind. Eng. Chem. Anal. Ed.* 9(2) (1937) 67–69.
- [21] APHA, AWWA and WEF, Standard methods for the examination of water and wastewater, twenty first ed., American Public Health Association (APHA), Washington DC, 2005, pp. 1–18.
- [22] Boletín Oficial de Canarias (BOC), Decreto 82/1999, BOC 73 (1999) 8382–8436.
- [23] M.A. Martín-González, O. González-Díaz, P. Susial, J. Araña, J.A. Herrera-Melián, J.M. Doña-Rodríguez, J. Pérez-Peña, Reuse of *Phoenix canariensis* palm frond mulch as biosorbent and as precursor of activated carbons for the adsorption of Imazalil in aqueous phase, *Chem. Eng. J.* 245 (2014) 348–358.
- [24] A. Nawaz, Z. Ahmed, A. Shahbaz, Z. Khan, M. Javed, Coagulation-flocculation for lignin removal from

- wastewater—A review, *Water Sci. Technol.* 69(8) (2014) 1589–1597.
- [25] H. Ganjidoust, K. Tatsumi, T. Yamagishi, R.N. Gholian, Effect of synthetic and natural coagulant on lignin removal from pulp and paper wastewater, *Water Sci. Technol.* 35(2–3) (1997) 291–296.
- [26] P.C. Bulson, D.L. Johnstone, H.L. Gibbons, W.H. Funk, Removal and inactivation of bacteria during alum treatment of a lake, *Appl. Environ. Microbiol.* 48(2) (1984) 425–430.
- [27] O. Bayat, V. Arslan, B. Bayat, C. Poole, Application of a flocculation–ultrafiltration process for bacteria (*Desulfovibrio desulfuricans*) removal from industrial plant process water, *Biochem. Eng. J.* 18(2) (2004) 105–110.
- [28] M. Abdollahi, Hydrogen peroxide, in: P. Wexler, *Encyclopedia of Toxicology*, third ed., Elsevier Inc., London, 2014, pp. 967–970.
- [29] F.J. Millero, W. Yao, J. Aicher, The speciation of Fe(II) and Fe(III) in natural waters, *Marine Chem.* 50 (1995) 21–39.
- [30] F.J. Millero, Solubility of Fe(III) in seawater, *Earth Planet. Sci. Lett.* 154 (1998) 323–329.
- [31] N. Clarke, L.G. Danielsson, The simultaneous speciation of aluminium and iron in a flow-injection system, *Anal. Chim. Acta* 306(1) (1995) 5–20.
- [32] J. Kragten, *Atlas of metal-ligand equilibria in aqueous solution*, John Wiley & Sons, New York, NY, 1978, pp. 173.
- [33] J. De Laat, G.T. Le, B. Legube, A comparative study of the effects of chloride, sulfate and nitrate ions on the rates of decomposition of H₂O₂ and organic compounds by Fe(II)/H₂O₂ and Fe(III)/H₂O₂, *Chemosphere* 55(5) (2004) 715–723.
- [34] J. De Laat, G.T. Le, Effects of chloride ions on the iron(III)-catalyzed decomposition of hydrogen peroxide and on the efficiency of the Fenton-like oxidation process, *Appl. Catal. B Environ.* 66(1–2) (2006) 137–146.
- [35] M.C. Lu, Y.F. Chang, I.M. Chen, Y.Y. Huang, Effect of chloride ions on the oxidation of aniline by Fenton's reagent, *J. Environ. Manage.* 75(2) (2005) 177–182.
- [36] L.G. Devi, C. Munikrishnappa, B. Nagaraj, K.E. Rajashekhar, Effect of chloride and sulfate ions on the advanced photo-Fenton and modified photo-Fenton degradation process of Alizarin Red S, *J. Mol. Catal. A Chem.* 374–375 (2013) 125–131.
- [37] M.K. Wang, M.K. White, J.L. Hem, Influence of acetate, oxalate, and citrate anions on precipitation of aluminum hydroxide, *Clays Clay Miner.* 31(1) (1983) 65–68.
- [38] K. Nohara, H. Hidaka, E. Pelizzetti, Processes of formation of NH₄⁻ and NO₃⁻ ions during the photocatalyzed oxidation of N-containing compounds at the titania/water interface, *J. Photochem. Photobiol. A Chem.* 102 (1997) 265–272.
- [39] R.G. Zepp, B.C. Faust, Photochemistry of aqueous iron (III)–polycarboxylate complexes: roles in the chemistry of atmospheric and surface waters, *Environ. Sci. Technol.* 27 (1993) 2517–2522.
- [40] J. Hoigne, Y. Zuo, Formation of hydrogen peroxide and depletion of oxalic acid in atmospheric water by photolysis of iron(III)–oxalato complexes, *Environ. Sci. Technol.* 26 (1992) 1014–1022.
- [41] J.A. Zazo, J.A. Casas, A.F. Mohedano, M.A. Gilarranz, J.J. Rodríguez, Chemical pathway and kinetics of phenol oxidation by Fenton's reagent, *Environ. Sci. Technol.* 39 (2005) 9295–9302.
- [42] G.V. Buxton, C.L. Greenstock, W.P. Helman, A.B. Ross, Critical Review of rate constants for reactions of hydrated electrons chemical kinetic data base for combustion chemistry. Part 3: Propane, *J. Phys. Chem. Ref. Data* 17 (1988) 513–886.
- [43] D. Rubio, E. Nebot, J.F. Casanueva, C. Pulgarin, Comparative effect of simulated solar light, UV, UV/H₂O₂ and photo-Fenton treatment (UV-Vis/H₂O₂/Fe^{2+,3+}) in the *Escherichia coli* inactivation in artificial seawater, *Water Res.* 47(16) (2013) 6367–6379.